

Optimization of Deposition Parameters on the Physical Properties of TiO₂ Thin Films by Spray Pyrolysis Technique

A. Gowri manohari¹, S. Dhanapandian^{1,*}, K. Santhosh Kumar¹ and T. Mahalingam²

¹ Department of Physics, Annamalai University, Annamalai Nagar – 608 002, India

² Department of Electrical and Computer Engineering, Ajou University, Suwon – 443 749, South Korea

Received: 7 Jun. 2013, Revised: 21 Sep. 2013, Accepted: 23 Sep. 2013

Published online: 1 Jan. 2014

Abstract: Titanium dioxide (TiO₂) thin films have been deposited on microscopic glass substrate by spray pyrolysis technique. The effect of deposition parameters such as substrate temperature, molarity (precursor concentration) and solution spray rate on the structural, surface morphological and optical properties of the films have been studied. The prepared films were characterized by X-ray diffraction (XRD), scanning electron microscope (SEM) with EDS and UV-Vis spectroscopy. The XRD patterns indicated that the films have amorphous and polycrystalline structure and the size of the crystallites have been changed from 9 to 48 nm. The optical band gap of the TiO₂ films is determined to be about 3.40 to 3.65 eV to the change of deposition conditions.

Keywords: Titanium dioxide; deposition parameters; spray pyrolysis; thin films

1 Introduction

TiO₂ is a promising, multifunctional semiconducting material and receiving much attention due to the ability of depositing films at lower temperature with atmospheric pressure and the non toxicity of the liquid precursors. The interest on titanium dioxide is mainly for its special properties like chemical stability [1, 2], photocatalytic potential [3], high dielectric constant ($\epsilon_r = 60 - 100$) [4, 5], increased electrical conductivity [6], favourable band gap [7] and high refractive index (2.6 – 2.9) [8]. Over the past decades TiO₂ films have been studied largely for their numerous applications, including catalysis, optical coatings, gas sensors, smart windows [9 – 11], dye sensitized solar cell [12], organic and inorganic absorber [13] and electrochromic devices [14]. Recently n-type TiO₂ thin films are also used for buffer layer material in solar cells. The applications of titania have been found to depend strongly on the crystalline structure, morphology and particle size [15, 16].

It is a relatively complex material and exhibited three polymorphic states: anatase (tetragonal), rutile (tetragonal) and brookite (orthorhombic). The parameters that affecting the phase of the films which are the

deposition method, deposition temperature, annealing temperature, deposition rate, deposition pressure, precursor type, reaction atmosphere, impurities present and type of the substrate. The anatase phase is obtained for the low temperature range of about 350 C and in the temperature between 400 and 800 C rutile phase was observed. At higher temperature, only the rutile phase is present whereas another possible phase brookite was just present at higher pressure with temperature. It has been found that the anatase structure with higher photocatalytic activity than rutile.

Many research groups have been synthesized the TiO₂ thin films by various methods such as molecular beam epitaxy [17], pulsed laser deposition [18], spin coating [19], chemical vapor deposition [20], reactive evaporation [21], vacuum evaporation [22], sputtering [23], chemical bath deposition [24], electrodeposition [25] and spray pyrolysis [26]. Among them spray pyrolysis is a simple, low cost and easily available technique for producing large area deposition with sufficient thickness in single step [27]. In this letter the preparation and characterization of TiO₂ thin films which are deposited on glass substrates using the spray pyrolysis technique is presented. The influence of the spray parameters like

* Corresponding author e-mail: dhanahockey@yahoo.co.in

substrate temperature, molarity and spray rate on the structural, surface morphology and optical properties of the films is also investigated.

2 Experimental details

Titanium dioxide (TiO₂) thin films were deposited on microscopic glass substrates using spray pyrolysis technique. A detailed description of the microcontroller based spray pyrolysis technique is given elsewhere [28]. The precursor solution was prepared by dissolving titanium tetra isopropoxide in 50 ml ethanol. To find the optimization of deposition parameters for the films (substrate temperature, precursor concentration and solution spray rate), three sets of films were prepared namely 'set 1', 'set 2' and 'set 3'. For all the sets, the deposited films under similar conditions: nozzle-to-substrate distance = 20 cm; carrier gas = air; carrier gas pressure = 1.0 kg/cm². 'Set 1', in order to study the effect of substrate temperature on the physical properties of the thin films, the substrate temperature was varied in the range of 375 – 475 C, with a step of 25 C. After optimizing the substrate temperature, 'Set 2' was prepared by varying the precursor concentrations from 0.05 – 0.15 M. In the 'set 3', to study the deposited films with different spray rate solution, the spray deposition was carried out at different rates in the range of 1 – 4 ml/min. Before deposited the films, the glass substrates were first cleaned with a water bath, followed by dipping in con.HCl, acetone and ethanol successively. Finally the substrates were rinsed in deionised water and allowed to dry in hot air oven. To prepare TiO₂ thin films with the conditions of spray deposition parameters are given in Table 1.

Table 1 Spray deposition parameters of TiO₂ thin films.

	Effect of substrate temperature (T _s)	Effect of variation of molarity (M)	Effect of spray rate (R)
Volume of spray solution (ml)	50	50	50
Substrate temperature (C)	375, 400, 425, 450, 475	475	475
Molarity (M)	0.1	0.05, 0.075, 0.1, 0.15	0.1
Spray rate (ml/min)	3	3	1, 2, 3, 4
Carrier gas pressure	1.0	1.0	1.0
Nozzle-to-substrate distance (cm)	20	20	20

Thickness of the films was measured using stylus method (Mitutoyo SJ 301). For the structural study was performed employing X-ray diffraction (XRD) by JEOL JDX-803 diffractometer using CuK α ($\lambda=1.5406$) radiation with 2θ in the range 20 - 60. The average crystallite size was calculated using Scherrer's formula

[29]:

$$D = \frac{K\lambda}{\beta \cos\theta} \quad (1)$$

where, K=0.94 is the shape factor, λ is the X-ray wavelength of CuK α radiation, θ is the Bragg's angle and β is the full width at half maximum of the peak. The lattice strain (ϵ) was calculated using the relation,

$$\epsilon = \frac{\beta \cos\theta}{4} \quad (2)$$

The values of dislocation densities (δ) were calculated using the relation,

$$\delta = \frac{15\epsilon}{aD} \quad (3)$$

The microstructural parameters such as crystallite size, micro strain and dislocation density of the films with various conditions have been summarized in Table 2.

The surface morphology of the films was studied by scanning electron microscopy (SEM) using JEOL JES-1600 with the magnification of 2K. Optical measurement of the films was carried out using a Varian-Cary 500 Scan UV-Vis-NIR double-beam spectrophotometer in the wavelength range of 300 – 1000 nm. The direct optical band gap (E_g) of the prepared films was obtained by optical absorption measurements and plotting $(\alpha h\nu)^2$ versus photon energy ($h\nu$) and using the relation [30]:

$$(\alpha h\nu)^2 = A (h\nu - E_g) \quad (??)$$

where, A is proportionality constant and E_g is the direct transition band gap.

3 Results and discussion

3.1 Structural properties

3.1.1 Effect of substrate temperature (T_s)

Figure 1 shows the XRD patterns of the TiO₂ films deposited with different substrate temperatures. The films prepared at T_s<400 C are mainly amorphous in nature. The previous works stated that the amorphous nature of TiO₂ films obtained at lower temperatures around 300 C [31, 32]. As the substrate temperature increased (T_s>400 C), the amorphous phase was partially crystallized into anatase TiO₂ phase. On increasing the temperature upto 475 C, the crystallinity of the film was further increased as confirmed from the intensity count of the peak. The presence of diffraction peak 25 is a highly preferential grain orientation along (??) axis with tetragonal crystal structure which indicated that the TiO₂ exists in the form of anatase phase. Hence we conclude that the crystalline formation is influenced by the substrate temperature. The

observed 2θ values were compared with standard data [33].

The structural parameters such as crystalline size, dislocation density and micro strain were determined from the appropriate equations and the values were shown in Table 2. With increasing the substrate temperature, the size of the crystallites (16.55 to 48.69 nm) is also increased [34]. From the table, it was generally observed that the strain and dislocation density in the film decreases as the crystallite size increases which is a well-known phenomenon [35].

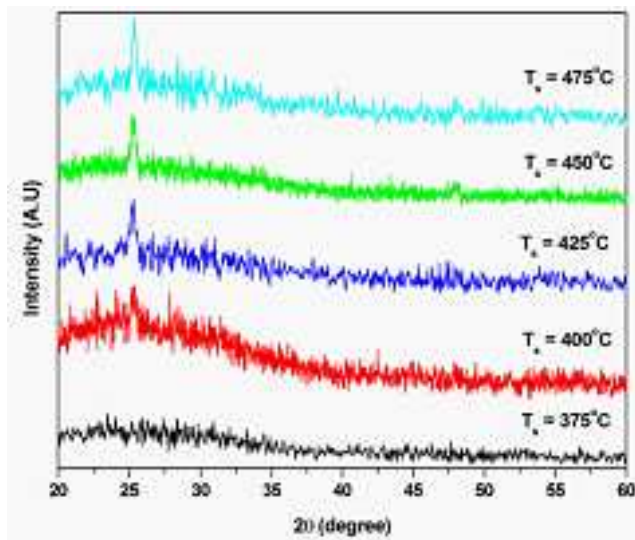


Figure 1 XRD patterns of TiO_2 thin films deposited at various substrate temperatures.

3.1.2 Effect of variation in molarity (M)

Figure 2 depicted the XRD patterns of TiO_2 films with various molarity. The films prepared with lower and higher precursor concentration of 0.05 and 0.125 M indicated an amorphous in nature. As the precursor concentration of 0.075 had formed the anatase phase as evident from the sample. It was found that the initiation of the crystalline phase occur at this concentration. The lower concentration (0.05 M) was insufficient for the crystallization of TiO_2 and at higher concentration (0.125 M) the temperature was insufficient for the crystallization. The solution concentration is great impact on the crystallization. The well defined reflections of the films could be indexed in terms of the anatase phase lattice was identified the precursor concentration of 0.1 M. The films had tetragonal crystal structure and oriented along (??) plane. Upon increasing the precursor concentration from 0.075 to 0.1 M, the crystallite size increased from 30.65 to 48.69 nm due to particle residence time [36].

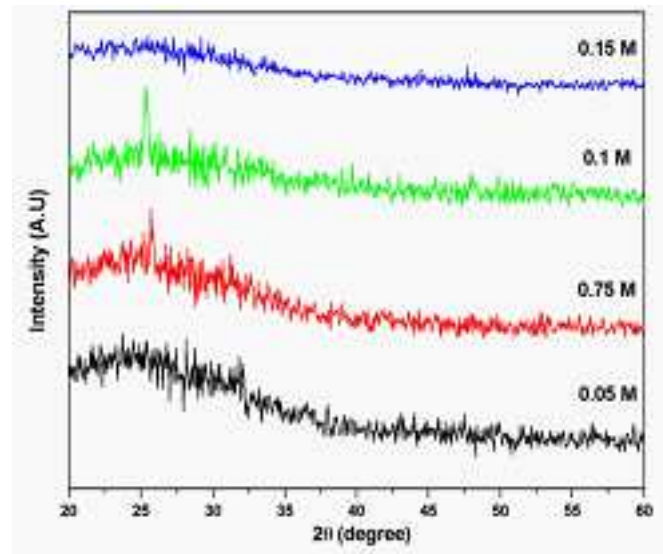


Figure 2 XRD patterns of TiO_2 thin films prepared at different molarities.

3.1.3 Effect of spray rate (R)

The XRD spectra of the films deposited at different spray rates are shown in Figure 3. The films prepared with a spray rate of 1 ml/min did not show any peaks of crystalline phase, which indicating the amorphous structure. The thermally activated transformation from an amorphous to anatase phase was depended on experimental parameters. The films prepared with spray rates of 2, 3 and 4 ml/min indicate a polycrystalline structure of anatase TiO_2 . Among them $R=3$ ml/min is the best spray rate for the highest structural order the degree of preferred orientation of the films varied largely with the deposition rate. Increasing the spray rate higher than 3 ml/min would lead to deterioration of intensity of (??) peak. Thus it was clear that the crystalline formation is influenced by the deposition rate. Crystallinity seems to be increased as the film thickness increases with increasing the spray rates from 1 to 4 ml/min. The size of the crystallites in the (??) plane of TiO_2 thin films is calculated for different spray rates and given in Table 2.

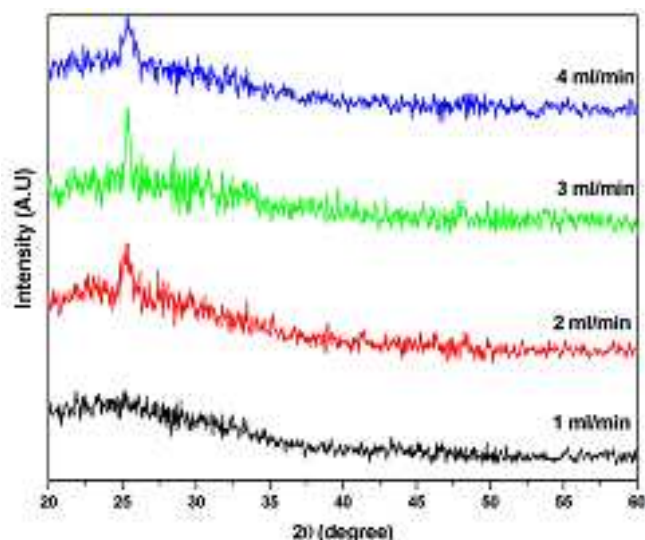


Figure 3 XRD patterns of TiO₂ thin films prepared at different spray rates.

Table 2 XRD results for Microstructural parameters of TiO₂ thin films.

	2θ (degree)	Crystallite size (nm)	Dislocation density (δ) x10 ¹⁴ lines/m ²	Micro Strain (ε) x10 ⁻⁴
(a) Effect of substrate temperature (Molarity = 0.1 M, Spray rate = 3 ml/min)				
375 C	-	-	-	-
400 C	25.2564	16.55	36.509	20.937
425 C	25.2692	24.95	16.061	13.891
450 C	25.2706	27.60	13.128	12.561
475 C	25.3484	48.69	4.219	7.119
(b) Effect of variation of molarity (T _s = 475 C, Spray rate = 3 ml/min)				
0.05 M	-	-	-	-
0.075 M	25.4865	30.65	11.271	9.811
0.10 M	25.3484	48.69	4.219	7.119
0.125 M	-	-	-	-
(c) Effect of spray rate (T _s = 475 C, Molarity = 0.1 M)				
1 ml/min	-	-	-	-
2 ml/min	25.7852	13.18	42.628	27.488
3 ml/min	25.3484	48.69	4.219	7.119
4 ml/min	25.1275	9.17	61.634	39.483

The SEM images of the films deposited at (a) T_s = 400 C and (b) T_s = 475 C have been shown in Figure 4. It was observed that the homogeneous surface exists in the films and the morphologies of the films changed with the substrate temperature. As increasing the substrate temperature from 400 C (Fig. 4(a)) to 475 C (Fig. 4(b)), the particles were densely packed, smooth without any cracks, pinholes or voids. This strongly indicated that the high mechanical stability of the films. The poor crystallinity of the films grown at low temperatures is probably due to the lack of thermal evaporation for the nucleation of deposited atoms. Figure 5 shows the EDAX spectrum of the TiO₂ films prepared at optimized parameters (T_s = 475 C, M = 0.1, R = 3 ml/min). The

ratio of the atomic percentage of Ti and O was 35 at% and 65 at%, respectively. It was evident that the presence of the elements almost in the stoichiometric ratio.

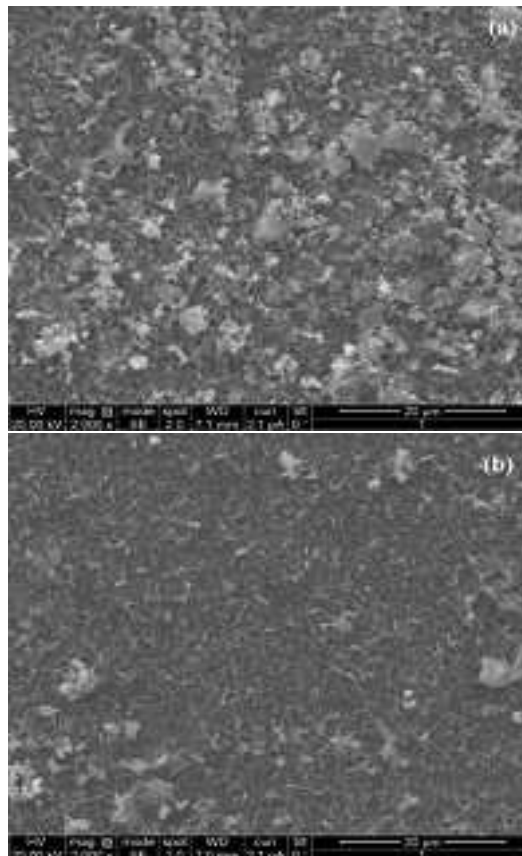


Figure 4 SEM image of TiO₂ films prepared at (a) T_s = 425 C and (b) T_s = 475 C.

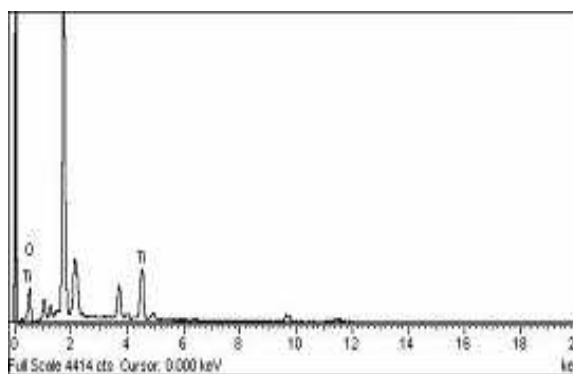


Figure 5 EDS spectrum of TiO₂ thin films prepared at T_s = 475C, Molarity = 0.1 M, Spray rate = 3 ml/min.

3.2 Optical properties

Figures 6 – 8 shows the optical band gap of the films in various deposition parameters is determined from the plot of $(\alpha h\nu)^2$ versus $h\nu$. The band gap energy was

determined by extrapolating the linear portion of the curve. The results of the optical properties of the films have been summarized in Table 3. These results indicated that with increasing the substrate temperature, the band gap values of films is decreased. This is due to the improvement in crystalline quality of TiO₂ thin films. This observation is fairly agrees with the XRD and SEM analysis. When increasing the molarity and spray rate leads to the increasing the optical band gap of films. The observed band gap values are good agreement with reported values between 3.2 – 3.9 eV [37]. Thicknesses of the films prepared at different substrate temperatures were measured and values were given in Table 3. From the table, it was observed that the thickness of the films decreased from 1045 nm to 655 nm with increase in substrate temperature. Such a decrease in thickness with increase in T_s for films fabricated using chemical spray pyrolysis has been reported earlier [38].

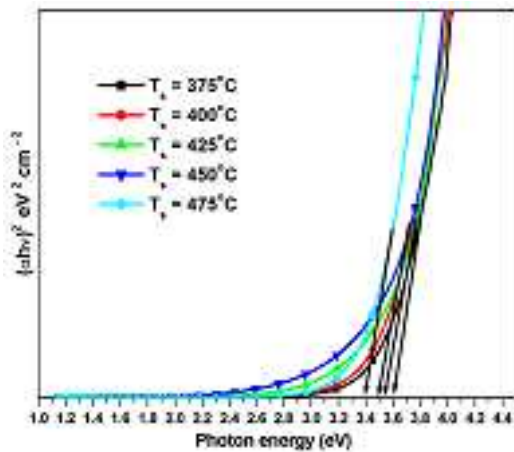


Figure 6 $(\alpha hv)^2$ versus photon energy (hv) of TiO₂ thin films deposited at different substrate temperatures.

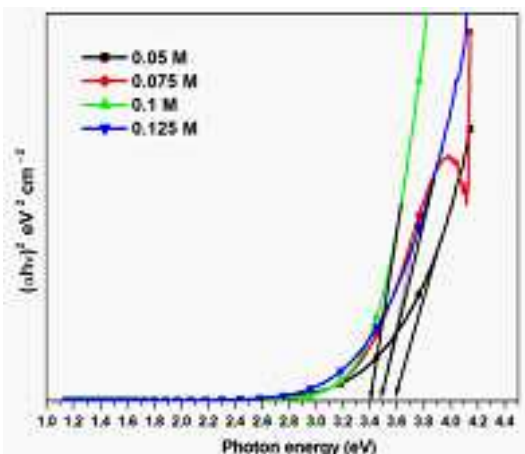


Figure 7 $(\alpha hv)^2$ versus photon energy (hv) of TiO₂ thin films prepared at different molarities.

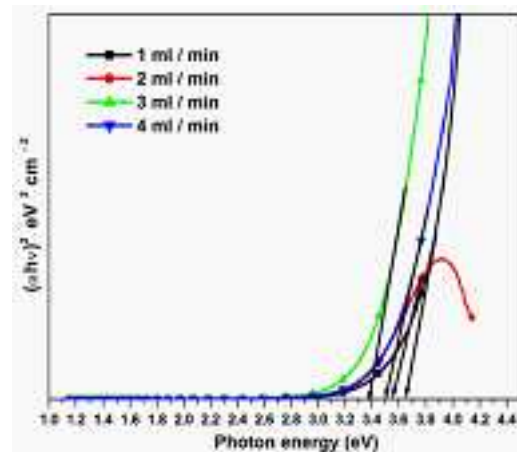


Figure 8 $(\alpha hv)^2$ versus photon energy (hv) of TiO₂ thin films prepared at different spray rates.

Table 3 Optical band gap values of TiO₂ thin films.

	E _g (eV)	Thickness (nm)
(a) Effect of T _s		
375 C	3.60	855
400 C	3.55	820
425 C	3.50	768
450 C	3.50	705
475 C	3.40	655
(b) Effect of M		
0.05 M	3.60	480
0.075 M	3.50	577
0.10 M	3.40	655
0.125 M	3.45	735
(c) Effect of R		
1 ml/min	3.65	524
2 ml/min	3.55	590
3 ml/min	3.40	655
4 ml/min	3.50	708

4 Conclusion

In this work, to find the deposition parameters for the preparation of TiO₂ films by spray pyrolysis technique were investigated. The substrate temperature, molarity and spray rate of solution such as 475 C, 0.1 M and 3 ml/min, respectively were optimized for TiO₂ films. The XRD studies indicated that the films were polycrystalline in nature with preferred grain orientation along (??) plane and exhibited tetragonal crystal structure. Optical band gap energy of the films revealed that the films can be fabrication of optical devices and solar cells.

References

[1] N.L. Wu, M.S. Lee and Z.J. Hsu, Journal of Photochemistry and Photobiology A: Chemistry, **163**, 277 – 280 (2004).

- [2] X.C. Zhang, H.Y. Wu, M.C. Zhu, E.Q. Wang and D.X. Li, *Advanced Materials Research*, **266**, 55 – 58 (2011).
- [3] M. Radeeka, M. Rekas, A. Trenczek-Zajac and K. Zakrzewska, *Journal of Power Sources*, **181**, 46 – 55 (2008).
- [4] M.K. Lee, H.C. Lee and C.M. Hsu, *Material Science in Semiconductor Processing*, **10**, 61 – 67 (2007).
- [5] K. Karthick, S. Kesavapandian and N. Victor Jaya, *Applied Surface Science*, **256**, 6829 – 6833 (2010).
- [6] K. Pomoni, A. Vomvas and Chr. Trapalis, *Journal of Non-Crystalline Solids*, **354**, 4448 – 4457 (2008).
- [7] N.F. Atta, H.M.A. Amin, M.W. Khalil and A. Galal, *International Journal of Electrochemical Science*, **6**, 3316 – 3332 (2011).
- [8] O. Carp, C.L. Huisman and A. Reller, *Progress in Solid State Chemistry*, **32**, 33 – 177 (2004).
- [9] B.R. Weinberger and R.B. Garber, *Applied Physics Letters*, **66**, 2409 – 2411 (1995).
- [10] D. Manno, G. Micocci, R. Rella, A. Serra, A. Taurino and A. Tepore, *Journal of Applied Physics*, **82**, 54 – 59 (1997).
- [11] C.G. Granqvist, *Applied Physics A*, **52**, 83 – 93 (1991).
- [12] B. O'Regan and M. Gratzel, *Nature*, **353**, 737 – 740 (1991).
- [13] K. Tennakone, G.R.R.A. Kumara, A.R. Kurrara Singhe, K.G.U. Wijayantha and P.M. Sirimane, *Semiconductor Science and Technology*, **10**, 1689 – 1692 (1995).
- [14] T.S. Kung, D. Kim and K.J. Kim, *The Journal of Electrochemical Society*, **145**, 1982 – 1986 (1998).
- [15] H. Lin, C.P. Huang, W. Li, C. Ni, S. Ismat Shah and Y.H. Tseng, *Applied Catalysis B: Environmental*, **68**, 1 – 11 (2006).
- [16] B. Gao, Y. Ma, Y. Cao, J. Zhao and J. Yao, *J. Solid State Chemistry*, **179**, 41 – 48 (2006).
- [17] Y. Gao, Y. Liang and S.A. Chambers, *Surface Science*, **365**, 638 – 648 (1996).
- [18] H.S. Yoon, S.K. Kim and H.S. Im, *Bulletin of the Korean Chemical Society*, **18**, 641 – 645 (1995).
- [19] A.R. Phani, M. Passacantando and S. Santucci, *Journal of Physics and Chemistry of Solids*, **63**, 383 – 392 (2002).
- [20] J. Aarik, A. Aidla, A.A. Kiisler, T. Uustare, J. Aarik and V. Sammelselg, *Thin Solid Films*, **305**, 270 – 273 (1997).
- [21] D. Mergel, D. Buschendorf, S. Eggert, R. Grammes and B. Samset, *Thin Solid Films*, **371**, 218 – 224 (2000).
- [22] N. Romeo, G. Sberveglieri and L. Tarricone, *Applied Physics Letters*, **32**, 807 – 809 (1978).
- [23] D.B. Fraser and H. Melchior, *Journal of Applied Physics*, **43**, 3120 – 3127 (1972).
- [24] N.R. Pavaskar, C.A. Menezes and A.P.B. Sinha, *Journal of the Electrochemical Society*, **124**, 743 – 748 (1977).
- [25] H.S. Potdar, R.I. Hegde, S. Badrinarayan and N. Pavaskar, *Solar Energy Materials*, **6**, 183 – 190 (1982).
- [26] I.S. Mulla, H.S. Soni, V.J. Rao and A.P.B. Sinha, *Journal of Materials Science*, **21**, 1280 – 1288 (1986).
- [27] P.S. Patil, *Materials Chemistry and Physics*, **59**, 185 – 198 (1999).
- [28] K. Santhosh Kumar, C. Manoharan, S. Dhanapandian and A. Gowri Manohari, *Spectrochimica Acta Part A: Molecular and Biomolecular Spectroscopy*, **115**, 840 – 844 (2013).
- [29] David R. Lide (Ed), *CRC Handbook of Chemistry and Physics*, CRC Press, Boca Raton, FL, (2005).
- [30] J. Bardeen, F.J. Blatt, L.H. Hall, *Proceedings of the Photoconductivity Conference, Atlantic City, Wiley, New York*, 146 (1956).
- [31] M.L. Hitchman and J. Zhao, *Journal de Physique IV France*, **9**, 357 – 364 (1999).
- [32] D. Leinen, J.P. Espinas, A. Fernandez and A.R. Gonzalez-Elipe, *Journal of Vacuum Science and Technology A*, **12**, 5 (1994).
- [33] JCPDS Card No. 21 – 1272.
- [34] A. Moses Ezhil Raj, V. Agnes, V. Bena Jothy, C. Ravidhas, Joachim Wollschlager, M. Suendorf, M. Neumann, M. Jayachandran and C. Sanjeeviraja, *Thin Solid Films*, **519**, 129 – 135 (2010).
- [35] A.S. Edelestein and R.C. Camarata, *Nanomaterials Synthesis Properties and Applications*, Institute of Physics Publishing, (1998).
- [36] N.S. Karan, A. Agarwal, P.K. Pandey, P. Smitha, S.J. Sharma, D.P. Mishra and N.S. Gajbhiye, *Materials Science and Engineering B*, **163**, 128 – 133 (2009).
- [37] H. Haug and S.W. Koch, *Quantum theory of the optical and electronic properties of semiconductors*, 3rd Edition, World Scientific Publishing Co. (1990).
- [38] K.L. Chopra and S.R. Das, *Plenum Press, New York*, (1983).